Inorganic Chemistry

pubs.acs.org/IC

Article

Accurate Ring Strain Energies of Unsaturated Three-Membered Heterocycles with One Group 13−16 Element

Alicia Rey Planells and Arturo Espinosa Ferao*

Cite This: *Inorg. Chem.* 2022, 61, 6459−6468

Read Online

ACCESS | Metrics & More | Article Recommendations | Supporting Information

ABSTRACT: High-quality ring strain energy (RSE) data for 1*H*-unsaturated $(CH)_2X$ parent rings, where X is a group 13−16 element, are reported in addition to the 2*H*-isomers of the pnictogenirene rings. RSE data are obtained from appropriate homosdesmotic reactions and calculated at the DLPNO-CCSD-(T)/def2-TZVPP//B3LYP-D3/def2-TZVP(ecp) level. 1*H*-Tallirene and 1*H*-plumbirene have unique donor−acceptor structures between an acetylene π(CC) orbital and an empty p orbital of a metallylene subunit (a Dewar−Chatt−Duncanson description) and therefore cannot be described as proper rings but as pseudocyclic structures. Also, 1*H*-indirene and 1*H*-oxirene lack ring critical points and constitute borderline cases of pseudorings. 1*H*-Unsaturated rings exhibit enhanced RSE compared to their saturated homologues. The mechanism of ring strain relaxation by increasing the s character in the lone pair (LP) of group 15−16 elements is remarkable and increases on descending the groups. Furthermore, RSE is affected by the aromatic character of group 13 rings and certain aromatic or antiaromatic character in group 14 or 15−16 rings, respectively, which tend to vanish on descending the group as shown by NICS(1) values. 2*H*-Unsaturated rings were found only for group 15 elements (although only 2*H*-azirine shows a proper cyclic structure) and displayed lower RSE (higher stability) than the corresponding 1*H*-isomers.

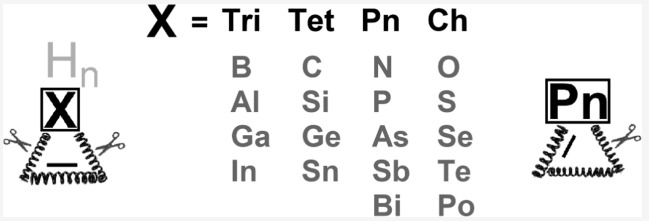

INTRODUCTION

The chemistry of unsaturated three-membered heterocycles has been an important field of study for theoreticians and experimentalists for decades. Their peculiar geometrical characteristics lie in their inherent high ring strain and the presence of unsaturated bonds and heteroatoms, which introduce (de)stabilizing factors such as lone pair repulsion, σ-aromaticity, delocalization, and rehybridization.[1] They are also a source of starting materials for the synthesis of a wide range of other more complex substances. For instance, the versatile cyclopropene is used as a reagent in the well-known Diels−Alder reactions[2] or in its chiral version to produce enantiomerically enriched methylene- and alkylidenecyclopropane derivatives.[3] Also, 2*H*-azirine is an important intermediate for the preparation of acyclic amino compounds[4] and substituted aziridines,[5] among other important reactions. And dimerization of borirene leads to 1,4-diboracyclohexadiene.[6]

In the study of three-membered unsaturated heterocycles containing (at least) a group 13−16 heteroatom, the essential concept of aromaticity (or antiaromaticity in case) in chemistry comes into play.[7] Numerous studies are reported in the literature that try to elucidate how this condition affects the geometrical and electronic aspects of this type of rings. Although the combination of acetylene and silylene was suggested to be an appropriate way of describing silacyclopropane (silirane), the stability exhibited when successfully synthesized by Seyferth in 1972[8] hinted at considering that its unsaturated version, silacyclopropene (1*H*-silirene), might also be stable due to some predicted aromatic character,[9] as a few years later demonstrated by the synthesis of the tetramethyl-1-silacycloprop-2-ene derivative by Conlin et al.[10] The heavier analogues 1*H*-germirenes were reported to be stable species,[11] and a high ring strain energy (RSE) of 44.4 and 47.6 kcal/mol were computed for the parent and 1-bromo-substituted rings,[12] respectively, whereas a somewhat lower strain was obtained for the corresponding 1*H*-silirene (RSE = 40.6 and 42.0 kcal/mol, respectively). On the other hand, the rather unstable 1*H*-thiirene was the first formally antiaromatic (4π electron) heterocycle prepared,[13] which tries to alleviate this destabilization by lengthening the C−S bonds and shortening the C═C bond. No less interesting is 1*H*-oxirene, which has given rise to considerable controversy as to whether the C_{2v}-symmetric structure exists as a local minimum or a saddle point energy between two degenerated low-symmetry (C_s) minima, which greatly turned out to depend on the computational level used.[14] However, it seems unanimous that its derivative dimethyloxirene does constitute a high-symmetry (C_{2v}) energy minimum.[15] As for the antiaromatic pnictogens

Received: January 7, 2022
Published: April 20, 2022

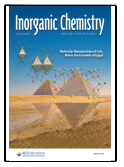

group, the three-membered N- and P-containing unsaturated rings constitute exciting fields in heterocyclic chemistry. The chemistry of aziridines and azirines has been a tremendously exploited field since the review of Padwa and Woolhouse.[16] Two types of azirines can be formed, namely, 1*H*-azirine and 2*H*-azirine, both exhibiting unique reactivity such as the ability to act as either nucleophile or electrophile,[17] as well as the possibility of being used as precursors to more complex N-containing molecules.[4] Their structures have been well studied recently.[18] A 2*H*-azirine is the highly strained key intermediate in the Neber rearrangement that transforms ketoximes into α-amino-ketones.[19] In contrast, the development of the chemistry of three-membered P-containing rings was somewhat delayed, starting with Wagner's discovery of phosphirane in 1963.[20] A few years later, 1*H*-phosphirene and 2*H*-phosphirene were discovered by Mathey[21] and Regitz,[22] respectively, both fields growing rapidly to become key building blocks in organophosphorus chemistry.[23] But it is not all about antiaromaticity: in 1998, the remarkable stability of 2π-electron aromatic 1*H*-borirene was reported to be the most stable isomer of BC_2H_3, in contrast to its aluminum counterpart, which highlights the ability of the B atom to form stable rings.[24]

In the present work, high-quality benchmark RSE (ring strain energy) data are reported for parent $(CH)_2X$ rings, where X is a group 13−16 element (Figure 1), with its most

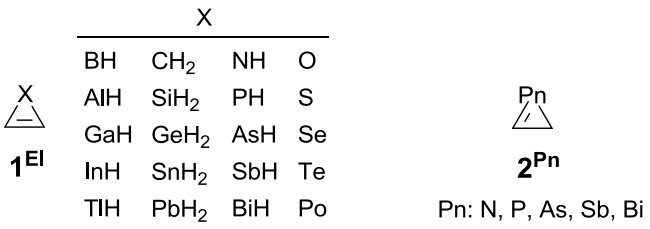

Figure 1. 1*H*- (**1**) and 2*H*-unsaturated (**2**) three-membered heterocycles studied.

characteristic covalency (3, 4, 3, and 2 for groups 13−16, respectively) completed by bonds with H, and is designated as $\mathbf{1}^{El}$ ("El" refers to the heavy element of group X). In addition, a discussion of possible factors affecting the ring strain as well as (anti)aromaticity in each case is presented. The 2*H*-isomers **2** were also studied, although only those with pnictogen atoms were found as stable species.

RESULTS AND DISCUSSION

1*H*-Unsaturated Ring Structures, 1. The main geometrical parameters for all computed (see the Experimental Section) energy minima of rings $\mathbf{1}^{El}$ (Figure 1) were collected (Table 1) to obtain an appropriate description of their structures.

The C═C bond distance maintains a general tendency to decrease on moving right within the row, probably due to the increasing electronegativity of the heteroatom, as also observed for the fully saturated counterparts and tested on simple acyclic $X-CH_2-CH_2-X$ model species (X = BH_2, CH_3, NH_2, OH).[25] On descending within the same group, the C═C bond distance decreases regularly, reaching limiting values (also very acute C−X−C bond angles) for rings containing heteroatoms with the highest metallic character Tl and Pb. Thus, $\mathbf{1}^{Tl*}$ (1*H*-thallirene) and $\mathbf{1}^{Pb*}$ (1*H*-plumbirene) present a pseudocyclic structure (designated with the asterisk) according to the

Table 1. Calculated (B3LYP-D3/def2-TZVPecp) C═C Bond Distances (Å) and C−X−C Bond Angles (Degrees, in Parentheses) for Compounds $\mathbf{1}^{El}$

group 13	group 14	group 15	group 16
B 1.346 (54.6)	**C** 1.287 (50.6)	**N** 1.269 (49.5)	**O** 1.269 (48.0)
Al 1.369 (43.3)	**Si** 1.330 (43.1)	**P** 1.292 (41.1)	**S** 1.271 (40.1)
Ga 1.356 (41.8)	**Ge** 1.319 (40.1)	**As** 1.287 (37.8)	**Se** 1.268 (36.8)
In 1.330 (36.1)	**Sn** 1.320 (36.3)	**Sb** 1.287 (34.3)	**Te** 1.267 (33.4)
Tl 1.201 (22.2)	**Pb** 1.203 (23.7)	**Bi** 1.280 (32.4)	**Po** 1.261 (31.5)

Dewar−Chatt−Duncanson (DCD) model,[26] where the HCCH moiety displays a high triple-bond (acetylene) character (WBI = 2.936 and 2.868 for $\mathbf{1}^{Tl*}$ and $\mathbf{1}^{Pb*}$, respectively). Hence, these pseudorings are better described by a dative bonding from a filled π(C≡C) orbital in an acetylene subunit to an empty p atomic orbital (AO) in the X (TlH or PbH_2) subunit (Figure 2). The energies correspond-

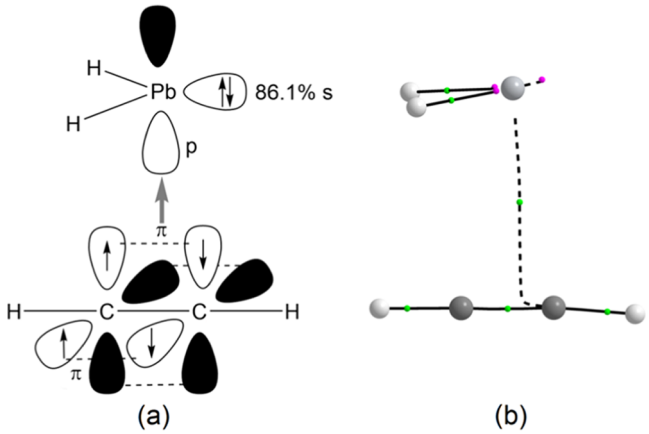

Figure 2. Sketched representation of DCD interaction (a) and computed (B3LYP/def2-TZVPPecp) structure with BCP (small green spheres), nuclear nonattractive critical points (NNACP, small pink spheres), and bond paths (b) for pseudo-plumbirene ($\mathbf{1}^{Pb*}$).

ing to this interaction, obtained from the second-order perturbation theory (SOPT) of the Fock matrix in the natural bond orbital (NBO) basis, for pseudo-thallirene and -plumbirene are 6.28 and 22.84 kcal/mol, respectively. Atoms-in-molecules (AIM) analysis[27] also supports this description by lacking a ring critical point (RCP) and attributing a single bond critical point (BCP) between the organic and metallic fragments (see Figures 2 and S1). This different behavior exhibited by $\mathbf{1}^{Tl*}$ and $\mathbf{1}^{Pb*}$ could be attributed to the well-known inert pair effect, typical for this type of post-transition-metal elements, which affects the tendency of the pair of the outermost s electrons not to be shared, making more favorable a structure with DCD-type interaction between two subunits.

1*H*-Indirene ($\mathbf{1}^{In*}$) represents a borderline case as it does not show a typical DCD structure due to the double C−C bond character (Table 1) (WBI = 2.028; natural localized molecular orbitals NLMO-BO = 2.007), but it can be categorized as a pseudocycle as it lacks RCP, only displaying one BCP at the shorter C−In bond (2.063 Å) and being the other slightly elongated (2.210 Å) (see the Supporting Information).

On the other hand, for the controversial oxirene $\mathbf{1}^{O*}$ geometry (*vide supra*), it was found that at the MP2(FU)/6-

https://doi.org/10.1021/acs.inorgchem.2c00067
Inorg. Chem. 2022, 61, 6459−6468

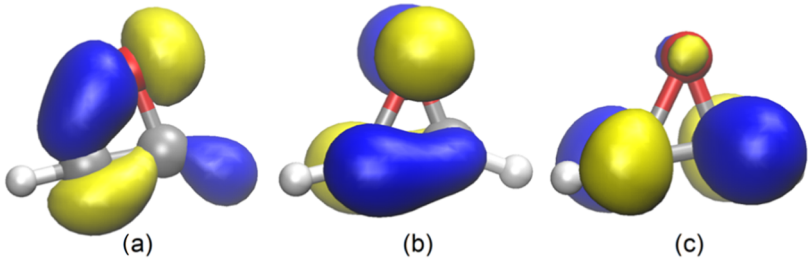

Figure 3. Computed (B3LYP-D3/def2-TZVP) Kohn−Sham isosurfaces (0.07 au) for (a) HOMO − 1, (b) HOMO, and (c) LUMO of pseudo-oxirene ($\mathbf{1}^{O}$*).

31G(d) level or using GGA functionals (BLYP, BP91, PBE, HCTH, HCTH147, and HCTH407), with various double- and triple-ζ quality basis sets with a variety of extra polarization functions, the C_{2v}-symmetric $\mathbf{1}^{O}$ constitutes a transition state (TS) between two degenerate low-symmetry (C_s) minima, whereas at the HF/6-31G(d) level, C_{2v}-$\mathbf{1}^{O}$ is a true minimum; for hybrid functionals (B3LYP, B3P91, PBE0, B97, B97-1, and B3P86), a disparity of results was obtained.[28] We have obtained similar results with the PBEh-3c[29] functional to those with HF calculations. At the working level of theory used for optimizations throughout the current study (see the Computational Details section), oxirene $\mathbf{1}^{O}$* has a C_s symmetry distorted structure with long (C_1−O 1.673 Å) and short (C_2−O 1.376 Å) bonds, interconverting through a very low-lying C_{2v}-symmetric TS ($\Delta\Delta E_{ZPE}^{\ddagger}$ = 0.28 kcal/mol). The weak and long C_1−O bond is due to the fact that it is formed involving two almost pure p AO at carbon (94.3% p) and oxygen (96.6% p), as shown in the highest occupied molecular orbital (HOMO) − 1 isosurface, with HOMO and lowest unoccupied molecular orbital (LUMO) displaying π*(C−O) and π*(C−C) character, respectively (Figure 3). However, oxirene lacks a ring critical point (RCP) therefore being categorized as a pseudocyclic structure.

Ring Strain Energy Values and Related Parameters for Compounds 1. Ring strain is one of the most remarkable aspects of small rings as it is closely linked to chemical reactivity and has been found to affect properties such as the stereochemical stability of $\sigma^3\lambda^3$-pnictogen ring atoms.[30] It frames the driving force for a ring to be transformed into open-chain products.[31] RSEs were calculated using homodesmotic reactions (reaction class 4 or "RC4"), which constitute the penultimate type in a hierarchy of increasingly accurate processes, due to the conservation of larger fragments, according to a recent classification and redefinition of reaction types used in thermochemistry.[32] Good estimates for RSE concerning saturated[25,31,33] and unsaturated[12,34] three-membered heterocycles were obtained according to this type of thermochemical reaction schemes. The highest ranked hyper-homodesmotic reactions (reaction class 5 or "RC5") were skipped because they have been shown to give rise to very similar RSE data to RC4,[25] but being somewhat problematic in some cases by introducing undesired noncompensated interactions due to the presence of longer chains. Therefore, the RSE for unsaturated three-membered $(CH)_2X$ heterocycles with group 13−16 heteroelements $\mathbf{1}^{El}$ was calculated using the RC4 scheme (Scheme 1) and obtained as the average of the opposite energy (including the zero-point energy correction) for the three bond cleavage reactions corresponding to the three endocyclic bond-breaking reactions (one C═C and two C−X bonds) (Table 2). Although in principle, the *Z*-isomer of

Scheme 1. Homodesmotic (RC4) Ring-Opening Reactions Used for the Estimation of RSE for $\mathbf{1}^{El}$

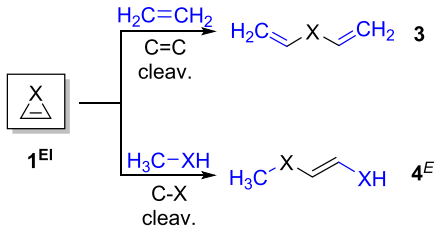

the homodesmotic C−X bond cleavage product should be the most suitable diastereomer according to its similarity with the endocyclic C═C bond, it introduces undesirable long-distance steric clashes, and hence only the *E*-isomer was used. The introduction of a C═C double bond in a small 3MR is expected to drastically increase the ring strain owing to the higher energy that should be required to compress an acyclic C═C−El bond angle from *ca.* 120° to the *ca.* 60° expected in the three-membered cyclic species, compared to the shorter bond angle compression required in a saturated C−C−E moiety. This is long time known since the first report of RSE for cyclopropene (53.2 kcal/mol)[35a] in 1976, compared to that of cyclopropane (27.9 kcal/mol).[25]

Data collected in Table 2 are in reasonable agreement with previously reported RSE data that were obtained using different computational levels and, in most cases, lower-quality thermochemical equations (*e.g.*, isodesmic reactions). Worth is mentioning the erroneously reported value of 34.5 kcal/mol for the RSE of $\mathbf{1}^{Si}$, which was referenced to a publication where this was not mentioned.[35c] On the other hand, the extremely high RSE value reported for the 1*H*-borirene $\mathbf{1}^{B}$ ring is based on the wrong assumption that an increase from the saturated counterpart borirane (reported RSE = 43.7 kcal/mol) could be estimated from the RSE difference (Δ_{RSE} = 24.8 kcal/mol) between cyclopropene ($\mathbf{1}^{C}$) and cyclopropane.[36]

For those (pseudo)rings with a diagnostic T1, a parameter widely used to evaluate the multi- or single-reference character, close to 0.02 (no ring or pseudo-ring exceeds this value). the multireference RSE value has been calculated by selecting the appropriate number of *n* electrons and *m* active orbitals (Table S3) to analyze possible differences between the two methods. The lowest values of single-reference contribution are shown for 1*H*-unsaturated $\mathbf{1}^{In}$* (76.2%) and $\mathbf{1}^{O}$* (80.6%) both with the highest diagnostic value T1 (0.02), although the RSE values for the two methods are quite similar for $\mathbf{1}^{In}$* (despite having considerable multireference character). The pseudo-ring $\mathbf{1}^{O}$* has a marked multireference character (of almost 20%), and this is reflected in a difference of about 5 kcal/mol between the two calculation methods.

https://doi.org/10.1021/acs.inorgchem.2c00067
Inorg. Chem. 2022, 61, 6459−6468

Table 2. RC4-Derived Calculated (DLPNO-CCSD(T)/def2TZVPPecp) RSE Values (kcal/mol) for Compounds 1^{El} and 2^{Pn}

1^{El}				2^{Pn}
group 13	group 14	group 15	group 16	group 15
B 31.15 (68.8[36c])	**C** 53.97 (53.2,[35a] 55.0,[35b] 55.5,[35c] 54.1,[35d] 55.7,[35e] 54.1,[35f] 54.1,[35g] 56.0[37])	**N** 71.02 (77.3[37])	**O**[b] 76.10 [71.31][a] (74.9,[35f] 82.4[37])	**N** 41.19 (43.9,[37] 41.9[38])
Al 42.09	**Si** 41.94 (45.5,[35b] 34.5,[35cc] 49.0[39])	**P** 38.03 (39.0[37])	**S** 51.51	**P**[b] 32.57 [31.38][a] (34.3[37])
Ga 45.46	**Ge** 46.62 (44.4[12])	**As** 35.89	**Se** 45.25	**As**[b] 32.73 [32.95][a]
In[b] 46.22 [46.29][a]	**Sn** 45.01	**Sb** 30.95	**Te** 38.15	**Sb**[b] 30.91 [29.71][a]
		Bi 26.92	**Po** 33.17	**Bi**[b] 28.12 [28.11][a]

[a]Values calculated at the CASSCF(*n*,6)/MRACPF/def2-SVPD level are presented in square brackets (see the Supporting Information for the specific number of active orbitals used, *n*). [b]Pseudocyclic structures. [c]See text.

As described in the previous section, the pseudocyclic oxirene ring $\mathbf{1}^{O*}$ lacks an RCP and exhibits an extremely high RSE value (that should be taken with caution), paralleling the high exothermicity of its low barrier ($\Delta E_{ZPE}^{\ddagger}$ = 3.63 kcal/mol) isomerization to ketene (ΔE_{ZPE} = −77.57 kcal/mol; reported: −80.02 kcal/mol[40]). Despite the similar high RSE value of 1*H*-azirine, $\mathbf{1}^{N}$, its proper cyclic structure is supported by the existence of BCPs for every endocyclic bond (see Table S1), as well as an RCP (Figure 4) with a high value of Lagrange

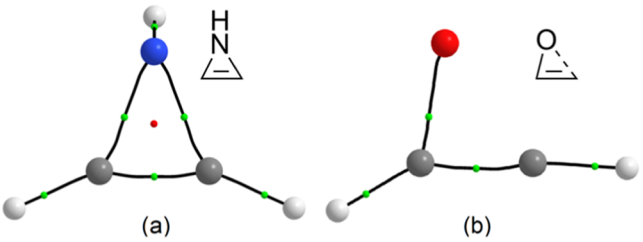

Figure 4. Computed (B3LYP/def2-TZVPP) BCP (small green spheres), RCP (small red sphere), and bond paths for (a) $\mathbf{1}^{N}$ and (b) $\mathbf{1}^{O*}$.

kinetic energy density per electron $G(r)/\rho(r)$ (see Table S1), which have been shown to correlate with RSE.[41] Moreover, calculation of the relaxed force constant,[42] a numerically stable and fully transferable parameter related to the stiffness of bond lengths or bond angles, reveals that the C−C−El bond angle of pseudocyclic $\mathbf{1}^{O*}$ (k^0 = 0.124 mdyn·Å) is below one-tenth of that for $\mathbf{1}^{N}$ (k^0 = 1.572 mdyn·Å), which also points to an inherent difference between pseudocyclic and cyclic characters, respectively.

Unsaturated rings with heteroatoms belonging to groups 15 and 16 experience the lone pair (LP) s character-enhancing effect on the RSE (Figure 5),[43] in line with the observed behavior of the already reported homologous saturated rings.[25] This increase of the LP s character causes the increase in p character for the AOs used by heteroatom "El" in the endocyclic C−El bonds, resulting in an sp^n-type hybridization with $n > 3$ (*i.e.*, beyond 75%p). As the s character of the LP AO increases on descending the group, the RSE for the corresponding heterocycle $\mathbf{1}^{El}$ decreases (Figure 5). The alternative plot of RSE against the p character of the AO used by the heteroatom "El" for its endocyclic C−El bonds, $\%p(El)_{C-El}$, shows a slightly worse correlation for groups 15 and 16 (R^2 = 0.8692 and 0.9826, respectively) (see Figure S4), while for groups 13 and 14, the expected almost constant p character (around 72 and 81%, respectively) is observed due to the absence of LPs.

Also, the relaxed force constants k^0 computed for C−El bonds in heterocycles with heaviest group 13−16 elements $\mathbf{1}^{El}$ parallels the behavior of RSE, as k^0_{C-El} decreases (bond elasticity increases) with the increase of $\%p(El)_{C-El}$ (Figure S2). The lighter elements (except C) fall out of the correlation, exhibiting unexpectedly low (for N and O) or high (for B) k^0_{C-El} values. For groups 13 and 14, the C−El bond stiffness is higher than for groups 15 and 16, and its decrease on moving down the group is much more pronounced. In the case of $\mathbf{1}^{O*}$ and $\mathbf{1}^{In*}$, both $\%p(El)_{C-El}$ and k^0_{C-El} are averaged values for the two different C−El bonds in the pseudo-ring. Furthermore,

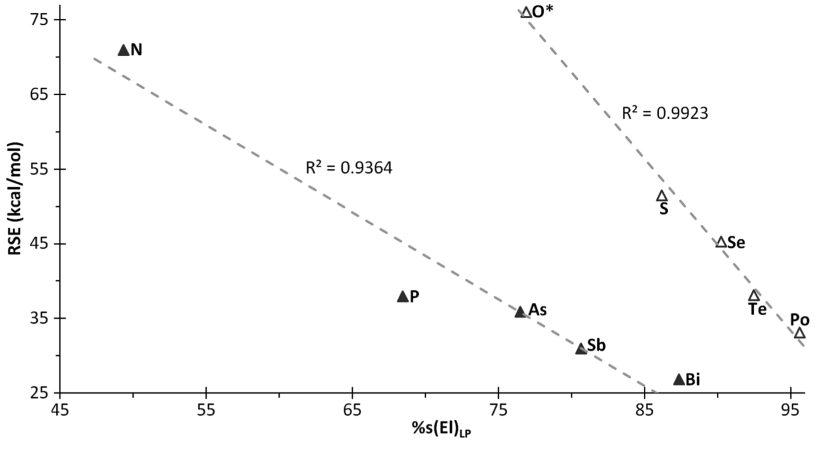

Figure 5. Plot of RSE *vs* s character (%) of AO used by pnictogen and chalcogen heteroatoms "El" lone pairs (LPs) in **1**.

https://doi.org/10.1021/acs.inorgchem.2c00067
Inorg. Chem. 2022, 61, 6459−6468

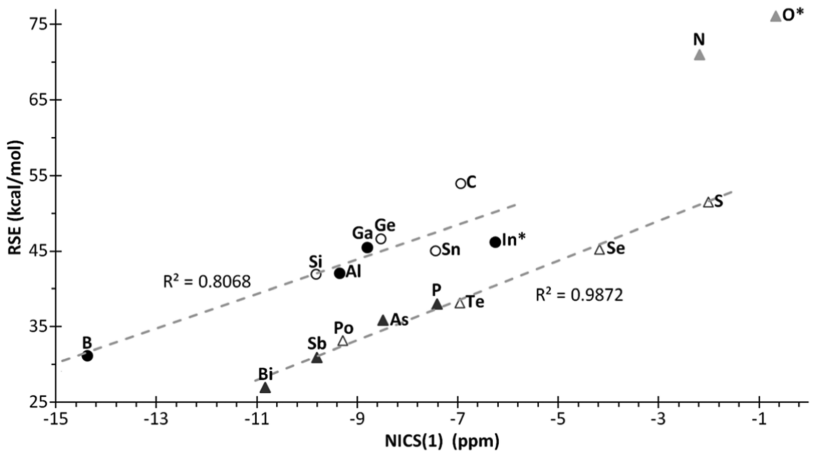

Figure 6. Plot of RSE *vs* computed (B3LYP/6311+G(d,p) or def2-TZVPP) NICS(1) (ppm) for compounds **1**. Excluding $\mathbf{1}^{N}$ and $\mathbf{1}^{O*}$ from the linear correlation.

due to the orthogonality of p AOs, an increase of p character should move the electron density of the σ(C−El) bond out of the hypothetical C−El straight bond line. Indeed, bond bending from NHO (natural hybrid orbital) directionality analysis shows a remarkable correlation between the deviation angle and the $\%p(El)_{C-El}$, only for group 15 and 16 elements (Figure S3). The angular deviation increases on moving down the group, being more pronounced (higher slope) for chalcogens than for pnictogens. This is indeed the opposite trend observed for RSE *versus* $\%p(El)_{C-El}$ (Figure S4), which suggests the easiness of bond bending as a mechanism for relieving the ring strain. For groups 13 and 14, the $\%p(El)_{C-El}$ values vary within a small range (*ca.* 70−74 and 79−82%, respectively) and, again, the angular deviation increases on descending the group (except for pseudocyclic $\mathbf{1}^{In*}$).

However, despite the strain-relieving effect of the LP s character in group 15−16 unsaturated heterocycles $\mathbf{1}^{El}$, the high RSE values displayed compared to their saturated counterparts (which represent the least strained rings within the series), and especially for $\mathbf{1}^{N}$ and $\mathbf{1}^{O}$ (also for $\mathbf{1}^{S}$ and $\mathbf{1}^{Se}$), are due to their intrinsic antiaromatic character or the geometric deformation to partially mitigate this electronic destabilization. In fact, the observed elongation of the endocyclic C−El bonds (Table S1) compared to analogous C−El bonds in acyclic species (taking the homodesmotic ring-opening products as a reference; see Table S2) is more pronounced for $\mathbf{1}^{N}$ (9.7%) and $\mathbf{1}^{O}$ (11.6% in average) and decreases significantly from the third period onwards ($\mathbf{1}^{P}$ 0.9%; $\mathbf{1}^{As}$ 1.2%; $\mathbf{1}^{Sb}$ 1.0; $\mathbf{1}^{Bi}$ 1.4%; $\mathbf{1}^{S}$ 5.8; $\mathbf{1}^{Se}$ 5.3; $\mathbf{1}^{Te}$ 4.6%; $\mathbf{1}^{Po}$ 4.6%), in accordance with the decreased antiaromaticity.

Although (anti)aromaticity is not an observable, several parameters have been described trying to quantify it from the geometrical, energetic, and magnetic perspectives.[44] One of the most widely used parameters is the nucleus-independent chemical shift (NICS)[45] which allows the aromatic character to be quantified so that the more negative the NICS value, the higher the aromatic character. As isotropic NICS values calculated at the ring centroid are strongly influenced by the σ-contributions,[46] NICS(1) (computed at 1 Å above and below the ring centroid) are usually employed.[47] The NICS(1) values for $\mathbf{1}^{El}$ were calculated at the standard B3LYP/6311+G(d,p) level[47] for elements of the second to fourth rows and using the def2-TZVPP basis set for elements of the fifth and sixth rows. At first sight, a clear correlation between NICS(1) and RSE is observed (Figure 6), with almost linear character for elements having (groups 15−16) or not having LPs (groups 13−14), if $\mathbf{1}^{N}$ and $\mathbf{1}^{O*}$ are excluded. As expected, the most antiaromatic rings are those with the lightest group 15−16 elements (nitrogen and oxygen) due to the most efficient overlap of the heteroelements LP with the π(C=C) orbital. Hence, antiaromaticity considerably decreases on moving down in groups 15 and 16 and varying almost linearly with RSE. As foreseeable, $\mathbf{1}^{B}$ is the most aromatic ring of all herein described,[48] therefore showing the most negative NICS(1) value and entailing a remarkable decrease in RSE (Figure 6). Again, on descending group 13, the heavier congeners of Al, Ga, and In use an empty p AO with increasing principal quantum number, which decreases the efficiency of the overlap with the C=C π-system, hence decreasing the aromaticity of the corresponding unsaturated heterocycles $\mathbf{1}^{El}$ and increasing their RSE.

As for group 14, it is worth mentioning the remarkable aromatic character, according to its highly negative NICS(1) value, observed for the $\mathbf{1}^{Si}$ ring (Figure 6), which has been explained in terms of using empty low-lying $3d_{xz}$ orbitals of silicon playing a similar role to the positive vacancy ($2p_z$) in the C atom of cyclopropenyl cation.[10] It should also be ascertained that the proposed[10] DCD-type structure for the 1*H*-silirene ring $\mathbf{1}^{Si}$, although suggested by the HOMO isosurface (Figure S5), must be ruled out, not only on the basis of its geometric features (Table 1) but also supported by the atoms-in-molecules (AIM) analysis,[27] showing three BCPs for the three endocyclic bonds and an RCP (Figure 7), and not a single BCP between the hypothetical acetylene and silylene moieties, as is would be expected for a DCD-type structure.

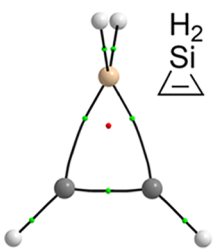

Figure 7. Computed (B3LYP/def2-TZVPP) BCP (small green spheres), RCP (small red sphere), and bond paths for $\mathbf{1}^{Si}$.

https://doi.org/10.1021/acs.inorgchem.2c00067
Inorg. Chem. 2022, 61, 6459−6468

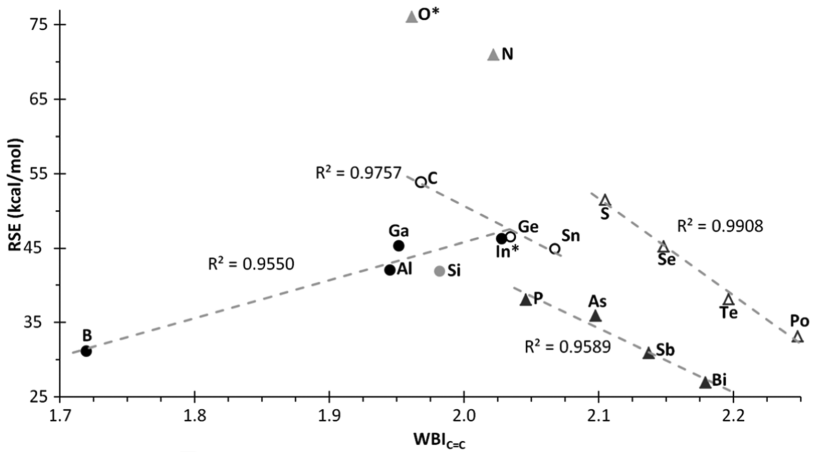

Figure 8. Plot of RSE *vs* $WBI_{C=C}$ for compounds **1**, excluding $\mathbf{1}^{Si}$, $\mathbf{1}^{N}$, and $\mathbf{1}^{O}$* from the linear correlation.

The aforementioned stabilization by d-orbital participation is supported by the NBO analysis, indicating E_{SOPT} = 3.88 kcal/mol associated with an electron transfer from a filled π(C═C) to an almost empty Si orbital with almost pure (95.9%) *d*-character. This SOPT energy in $\mathbf{1}^{Ge}$ (1.24 kcal/mol, 90.7% *d*-character) and $\mathbf{1}^{Sn}$ rings (1.10 kcal/mol, 69.5% *d*-character) decrease due to participation of 4d and 5d orbitals, respectively, with increasing energy gap, whereas $\mathbf{1}^{C}$ lacks d orbitals, which justifies its nonaromatic character. However, the origin of the diatropic ring current (aromaticity) accounting for the observed highly negative NICS(1) value for $\mathbf{1}^{Si}$ can mostly arise from an energetically more important sacrificial hyperconjugation effect between the π(C═C) and the two σ*(Si−H) molecular orbitals, each amounting to E_{SOPT} = 10.64 kcal/mol. The energy of the analogous double SOPT interaction decreases for the $\mathbf{1}^{Ge}$ and $\mathbf{1}^{Sn}$ rings (8.24 and 5.22 kcal/mol respectively), in line with their lower aromaticity. Similarly, for groups 15 and 16, whereas $\mathbf{1}^{N}$ and $\mathbf{1}^{O}$* lack d-orbitals, a small yet significant electron transfer is observed for $\mathbf{1}^{P}$ and $\mathbf{1}^{S}$ from π(C═C) to empty d-orbitals (82.3 and 60.4% *d*-character, respectively), the SOPT interaction amounting to 5.89 and 5.74 kcal/mol, respectively. This suggests a certain (small) aromatic component, which has an effect on a decrease of RSE and a more negative NICS(1) resulting from a small diatropic current. This effect decreases (lower E_{SOPT}) for heavier elements due to the increased energy gap between the donor π(C═C) orbital and the acceptor El-centered empty AO with increasingly lower *d*-character.[49] The reason for the increase in the aromaticity-related NICS(1) descriptor as one moves down in groups 15 and 16 is not trivial but could be tentatively explained on the basis of the increasing size of the heavier atoms, whose inner-shell electrons could give rise to heteroatom-centered diatropic currents that could interfere in the overall NICS(1) value. The use of NICS(2) values (computed 2 Å away from the ring centroid) did not provide a clearer picture, and the same trends were observed when plotted against RSE (see Figure S6), with good linear correlations within groups and all rings displaying lower negative values than benzene.[47] For group 15 rings, a decrease of sacrificial hyperconjugation of the π electron density with the σ*(El−H) molecular orbital on descending the group could also explain the decrease in aromaticity (E_{SOPT} = 8.54, 6.40, 4.61, and 3.59 kcal/mol for $\mathbf{1}^{P}$, $\mathbf{1}^{As}$, $\mathbf{1}^{Sb}$, and $\mathbf{1}^{Bi}$, respectively).

Nevertheless, as a consequence of the very high energy of the d-orbitals from the third row onward, the above-described effect of aromatic components could be negligible in this type of rings[50] and, instead, other substituent-depending hyperconjugation effects may come into play.

RSE may also be related to the strength of endocyclic bonds. Among bond-strength-related parameters, the widely used Wiberg bond index (WBI)[51] as well as the bond order provided by the Natural Localized Molecular Orbitals (NLMO)[52] analysis (NLMO-BO), less prone to overestimate the covalent character of the bond,[53] were computed for all $\mathbf{1}^{El}$ heterocycles. The representation of the RSE *versus* both WBI (Figure 8) and NLMO-BO (see Figure S7) of the C═C bond show that for groups 14−16, as the ring strain decreases when moving down the group, the C═C bond order increases, but without reaching a value close to a genuine triple-bond character as in the case of DCD-type pseudorings (WBI/NLMO-BO = 2.934/2.943 and 2.867/2.902 for $\mathbf{1}^{Tl}$* and $\mathbf{1}^{Pb}$*, respectively). For $\mathbf{1}^{In}$*, the WBI for the C═C bond (2.028) is clearly overestimated compared to the NLMO-BO (1.885), the latter falling out of the linear correlation of its group (Figure S7) probably because of its pseudocyclic character. 1*H*-Silirene $\mathbf{1}^{Si}$ is also markedly outside the linear correlation of group 14 (for both WBI and NLMO-BO), most likely due to its exceptional aromaticity with respect to the rest of the tetrel-based unsaturated rings, leading to a decrease in the RSE but without greatly affecting the strength of the C═C moiety. The most aromatic ring, 1*H*-borirene ($\mathbf{1}^{B}$), shows the lowest C═C bond orders (WBI = 1.720; NLMO-BO = 1.873) owing to the effective conjugation of the vacant p orbital in B to the C═C bond, drastically suppressed in the less aromatic and more strained $\mathbf{1}^{Al}$ and $\mathbf{1}^{Ga}$ rings (Figure 8).

In all, despite the expected large difference in RSE between 1*H*-unsaturated 3MRs and their saturated analogues, this turned out to be true only for $\mathbf{1}^{C}$. For the heaviest group 14 elements, this difference becomes less pronounced because of the aromatic stabilization of the unsaturated rings. By contrast, the aromatic stabilization of group 13 unsaturated rings results in a somewhat lower RSE than their saturated counterparts. In the case of group 15 and 16 heterocycles, the RSE of the unsaturated rings is much higher than that of their saturated counterparts due to the additional antiaromaticity destabilization effect.

2*H*-Unsaturated Three-Membered Rings 2. 2*H*-Unsaturated three-membered heterocycles ($\mathbf{2}^{El}$) were only found as

https://doi.org/10.1021/acs.inorgchem.2c00067
Inorg. Chem. 2022, 61, 6459−6468

energy minima for the elements of group 15 (2^{Pn}). The RSE data for these pnictogen-containing rings (Table 2) were calculated using the same type of homodesmotic reaction scheme as for the previously described rings (Scheme 2).

Scheme 2. Homodesmotic (RC4) Ring-Opening Reactions Used for the Estimation of RSE for 2^{Pn}

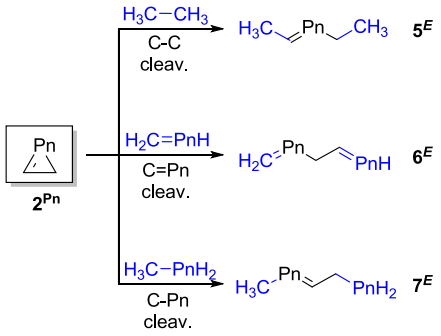

However, only the 2*H*-azirine ring, 2^{N}, contains three BCPs corresponding to the three endocyclic bonds and a proper RCP (Figure 9a), while neither BCPs for the single C−El bond

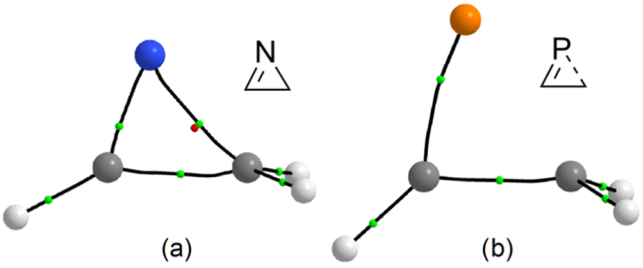

Figure 9. Computed (B3LYP/def2-TZVPP) BCP (small orange spheres) and bond paths for (a) 2^{N} and (b) 2^{P}*.

nor RCP were found for the rest of rings with heavier pnictogens. Taking 2^{P}* as a case in point, the lack of RCP and BCP(P−C) can be observed (Figure 9b); furthermore, 2^{P}* features a very elongated single C−P bond (1.906 Å) in comparison to the C−P single bond of the 1*H*-phosphirene 1^{P} isomer (1.840 Å) or to that in phosphirane (1.876 Å).[25] Consequently, except 2*H*-azirine (2^{N}), all heavier 2*H*-pnictogenirenes 2^{Pn}* must be considered pseudocyclic structures and their computed RSE used with caution. The analysis of the multireference RSE data calculated for these pseudorings (Table 2) shows that there is no significant difference with the single-reference (sr) data, even for 2^{Bi}* (84.3% sr) and 2^{Sb}* (86.5% sr) with a multireference contribution of about 15%.[54]

Recently, we have reported on the C=N bond-containing three-membered ring oxazirine.[34a] The latter could be considered either as oxa-analogue (replacement of $-CH_2-$ by $-O-$) of 2*H*-azirine (2^{N}), compared to which exhibits a somewhat enhanced RSE (44.28 kcal/mol), or as aza-analogue (replacement of =CH− by =N−) of pseudo-1*H*-oxirene (1^{O}*), displaying similar pseudocyclic structure due to the absence of RCP as a consequence of the elongated N−O bond (with no BCP).

It is worth mentioning the higher stability of the 2*H*-pnictogenirene rings 2^{Pn} compared to the corresponding 1*H*-isomers 1^{Pn}, as can be inferred from the variation in RSE (Table 2). This difference is very pronounced for the N-containing rings ($\Delta\Delta E_{ZPE}$ = 29.83 kcal/mol), mainly due to the antiaromatic character of 1^{N}. For heavier pnictogens, this difference becomes less noticeable ($\Delta\Delta E_{ZPE}$ = 5.46, 3.16, 0.04, and −1.20 kcal/mol for P, As, Sb, and Bi, respectively), probably due to the decrease of the antiaromatic character.

EXPERIMENTAL SECTION

Density functional theory (DFT) calculations were performed with the ORCA program.[55] All geometry optimizations were run in redundant internal coordinates in the gas phase, with tight convergence criteria, and using the B3LYP[56] functional together with Ahlrichs segmented def2-TZVP basis set[57] and the 2010 Grimme's semiempirical atom-pairwise London dispersion correction (DFT-D3).[58] From these geometries, all electronic data were obtained through single-point calculations (SP) using the same quality basis set but including additional polarization, def2-TZVPP.[59] Energy values were corrected for the zero-point vibrational term at the optimization level and obtained by the newly developed DLPNO method[60] for the "coupled-cluster" level with single, double, and triple perturbatively introduced excitations (CCSD(T)).[61] It is worth mentioning that the RI-JK speeding up approximation for Coulomb and Hartree−Fock (HF) exchange (in HF step for post-HF calculations) gave rise to anomalous results for fifth-row elements even when using appropriate auxiliary basis sets.[25] Therefore, this approach was skipped for all high-level RSE calculations. T1-Diagnostic values close to 0.02 prompted us to use dynamic correlation on top of the CASSCF(*n*,*m*) method[62] employing a (6,6) active space for 1^{In}* and 1^{O}*, whereas (8,6) for 2^{As}*, 2^{Sb}* and 2^{Bi}*, with the multireference average coupled-pair functional (MRACPF)[63] approach and the def2-SVPD basis set.[64] Analysis of the hybridization in the AO used for the endocyclic bonds was performed with the NBO method.[65] Properties derived from the topological analysis of the electronic density were obtained with the Multiwfn program,[66] whereas Figures 2b, 4, 7, and 9 were plotted with AIMall.[67] Figure 3 was drawn with Visual Molecular Dynamics (VMD).[68]

CONCLUSIONS

Accurate high-level (DLPNO-CCSD(T)/def2TZVPP//B3LYP-D3/def2TZVP) values were provided for the ring strain energy (RSE) in unsaturated three-membered rings containing only one 13−16 group element. A thorough exploration of the structural and electronic features of the 1*H*-unsaturated rings 1^{El} resulted in the classification of those with the most metallic elements, 1^{Tl}* and 1^{Pb}*, as pseudocyclic structures because of their typical Dewar−Chatt−Duncanson-type bonding lacking a ring critical point (RCP), 1*H*-indirene (1^{In}*) constituting a borderline case. At the working level of theory, the controversial C_{2v}-symmetric 1*H*-oxirene, 1^{O}, is a transition state (TS) between two low-symmetry (C_s) degenerate minima (1^{O}*) with pseudocyclic character. Among the 2*H*-unsaturated three-membered rings, 2^{El}, only found as a minimum for the pnictogen elements and presenting low RSE compared to the 1^{El} isomers, just 2*H*-azirine (2^{N}) presents a proper ring structure (*i.e.*, featuring an RCP).

RSE in groups 15 and 16 containing 1*H*-unsaturated rings 1^{El} is very much affected by the strain relaxation effect of the increased s character of one LP orbital of pnictogens and chalcogens, as already described for their saturated counterparts. The existence of an empty orbital in group 13 rings gives them the possibility of presenting a significant aromatic character, especially in the case of borirene 1^{B}. The existence of empty d orbitals in 1*H*-tetrelirenes, allows their use to

https://doi.org/10.1021/acs.inorgchem.2c00067
Inorg. Chem. 2022, 61, 6459−6468

acquire some aromaticity, especially in the case of 1*H*-silirene $\mathbf{1}^{Si}$, while moving down in the group the energy of these d orbitals increases, hence decreasing this aromatic contribution. On the other hand, the high antiaromaticity of $\mathbf{1}^{O}$* and $\mathbf{1}^{N}$, partially alleviated by geometric distortion, results in enhanced RSE. For the heavier group 15 and 16 elements, the antiaromaticity considerably decreases on descending the group, which together with the increase in heteroatom size and aromatic and/or hyperconjugative contributions result in a remarkable RSE decrease.

■ ASSOCIATED CONTENT

Supporting Information

The Supporting Information is available free of charge at https://pubs.acs.org/doi/10.1021/acs.inorgchem.2c00067.

Plots of the relaxed force constants and of the RSE *versus* other parameters; additional tables with electronic, structural, and bond strength parameters; as well as Cartesian coordinates and energies for all calculated species (PDF)

■ AUTHOR INFORMATION

Corresponding Author

Arturo Espinosa Ferao − *Departamento de Química Orgánica, Facultad de Química, Campus de Espinardo, Universidad de Murcia, 30100 Murcia, Spain;* orcid.org/0000-0003-4452-0430; Email: artuesp@um.es

Author

Alicia Rey Planells − *Departamento de Química Orgánica, Facultad de Química, Campus de Espinardo, Universidad de Murcia, 30100 Murcia, Spain*

Complete contact information is available at: https://pubs.acs.org/10.1021/acs.inorgchem.2c00067

Notes

The authors declare no competing financial interest.

■ ACKNOWLEDGMENTS

The authors thank the computation center at Servicio de Cálculo Científico (SCC—University of Murcia) for technical support and the computational resources used. Helpful discussions with Prof. L. Nyulászi are deeply acknowledged.

■ REFERENCES

(1) (a) Wiberg, K. B. The Concept of Strain in Organic Chemistry. *Angew. Chem., Int. Ed.* **1986**, *25*, 312−322. (b) Göller, A.; Clark, T. σ*-Aromaticity in Three-Membered Rings. *J. Mol. Model.* **2000**, *6*, 133−149. (c) *Reactive Intermediate Chemistry*; Moss, R. A.; Platz, M. S.; Jones, M., Jr., Eds.; John Wiley & Sons, 2004.

(2) Liu, F.; Paton, R. S.; Kim, S.; Liang, Y.; Houk, K. N. Diels-Alder Reactivities of Strained and Unstrained Cycloalkenes with Normal and Inverse-Electron-Demand Dienes: Activation Barriers and Distortion/Interaction Analysis. *J. Am. Chem. Soc.* **2013**, *135*, 15642−15649.

(3) Marek, I.; Simaan, S.; Masarwa, A. Enantiomerically Enriched Cyclopropene Derivatives: Versatile Building Blocks in Asymmetric Synthesis. *Angew. Chem., Int. Ed.* **2007**, *46*, 7364−7376.

(4) (a) Padwa, A.; Dharan, M.; Smolanof, J.; Wetmore, S. I. Photochemical transformations of small ring heterocyclic compounds. XLVI. Scope of the photoinduced 1,3-dipolar addition reactions of arylazirines. *J. Am. Chem. Soc.* **1973**, *95*, 1945−1954. (b) Palacios, F.; Aparicio, D.; de Retana, A. M. O.; de los Santos, J. M.; Gil, J. I.; Alonso, J. M. Asymmetric Synthesis of 2*H*-Azirines Derived from Phosphine Oxides Using Solid-Supported Amines. Ring Opening of Azirines with Carboxylic Acids. *J. Org. Chem.* **2002**, *67*, 7283−7288.

(5) Palacios, F.; de Retana, A. M. O.; de Marigorta, E. M.; de los Santos, J. M. Preparation, properties and synthetic applications of 2*H*-azirines a review. *Org. Prep. Proced. Int.* **2002**, *34*, 219−269.

(6) Budzelaar, P. H. M.; Van der Kerk, S. M.; Krogh-Jespersen, K.; Schleyer, P. v. R. Dimerization of Borirene to 1,4-Diboracyclohexadiene. Structures and Stabilities of $(CH)_4(BH)_2$ Molecules. *J. Am. Chem. Soc.* **1986**, *108*, 3960−3967.

(7) (a) Krogh-Jespersen, K.; Cremer, D.; Dill, J. D.; Pople, J. A.; Schleyer, P. v. R. Aromaticity in Small Rings Containing Boron and Carbon ($(CH)_2(BH)_n$, n = 1, 2). Comparisons with Isoelectronic Carbocations. The Decisive Roles of Orbital Mixing and Nonbonded 1,3-Interactions in the Structures of Four-Membered Rings. *J. Am. Chem. Soc.* **1981**, *103*, 2589−2594. (b) Gupta, R.; Bansal, R. K. Aromaticity/antiaromaicity of phospha-analoges of carbocyclic ions: A DFT investigation. *Comput. Theor. Chem.* **2016**, *1076*, 1−10.

(8) Lambert, R. L., Jr.; Seyferth, D. Substituted 7-siladispiro-(2.0.2.1)heptanes. The first stable silacyclopropanes. *J. Am. Chem. Soc.* **1972**, *94*, 9246−9248.

(9) Barthelat, J.-C.; Trinquier, G.; Bertrand, G. Theoretical investigations on some C_2SiH_4 isomers. *J. Am. Chem. Soc.* **1979**, *101*, 3785−3789.

(10) Conlin, R. T.; Gaspar, P. P. Tetramethylsilacyclopropene. *J. Am. Chem. Soc.* **1976**, *98*, 3715−3716.

(11) (a) Mizuhata, Y.; Sasamori, T.; Tokitoh, N. Stable Heavier Carbene Analogues. *Chem. Rev.* **2009**, *109*, 3479−3511. (b) Meiners, F.; Saak, W.; Weidenbruch, M. A Germacyclopropene with Electronegative Groups at the Ring Carbon Atoms. *Z. Anorg. Allg. Chem.* **2002**, *628*, 2821−2822. (c) Ishida, S.; Iwamoto, T.; Kira, M. Addition of a stable dialkylsilylene to carbon−carbon unsaturated bonds. *Heteroat. Chem.* **2011**, *22*, 432−437. (d) Lai, T. Y.; Guo, J.-D.; Fettinger, J. C.; Nagase, S.; Power, P. P. Facile insertion of ethylene into a group 14 element-carbon bond: effects of the HOMO−LUMO energy gap on reactivity. *Chem. Commun.* **2019**, *55*, 405−407.

(12) Sugahara, T.; Espinosa Ferao, A.; Rey Planells, A.; Guo, J.-D.; Aoyama, S.; Igawa, K.; Tomooka, K.; Sasamori, T.; Hashizume, D.; Nagase, S.; Tokitoh, N. 1,2-Insertion reactions of alkynes into Ge−C bonds of arylbromogermylene. *Dalton Trans.* **2020**, *49*, 7189−7196.

(13) Hess, B. A., Jr.; Schaad, L. J.; Ewig, C. S. An ab Initio SCF Study of the Structure and Vibrational Spectrum of Thiirene. *J. Am. Chem. Soc.* **1980**, *102*, 2507−2508.

(14) (a) Vacek, G.; Colegrove, B. T.; Schaefer, H. F., III Does oxirene exist? A theoretical inquiry involving the coupled-cluster method. *Chem. Phys. Lett.* **1991**, *177*, 468−470. (b) Vacek, G.; Galbraith, J. M.; Yamaguchi, Y.; Schaefer, H. F., III; et al. Oxirene: To Be or Not To Be? *J. Phys. Chem. A* **1994**, *98*, 8660−8665.

(15) Fowler, J. E.; Galbraith, J. M.; Vacek, G.; Schaefer, H. F., III Substituted Oxirenes (X_2C_2O, X = BH_2, CH_3, NH_2, OH, F): Can They Be Made? *J. Am. Chem. Soc.* **1994**, *116*, 9311−9319.

(16) Padwa, A.; Woolhouse, A. D. *Comprehensive Heterocyclic Chemistry*; Katritzky, A. R.; Rees, C. W., Eds.; Pergamon Press: Oxford, 1984; Vol. 7.

(17) Padwa, A. Azirine Photochemistry. *Acc. Chem. Res.* **1976**, *9*, 371−378.

(18) Császár, A. G.; Demaison, J.; Rudolph, H. D. Equilibrium Structures of Three-, Four-, Five-, Six-, and Seven-Membered Unsaturated N-Containing Heterocycles. *J. Phys. Chem. A* **2015**, *119*, 1731−1746.

(19) (a) Neber, P. W.; Friedolsheim, Av. Über eine neue Art der Umlagerung von Oximen. *Justus Liebigs Ann. Chem.* **1926**, *449*, 109−134. (b) O'Brien, C. The Rearrangement of Ketoxime O-Sulfonates to Amino Ketones (The Neber Rearrangement). *Chem. Rev.* **1964**, *64*, 81−89.

(20) (a) Wagner, R. I. U.S. Patent US3086053 and 3086056. (b) Wagner, R. I.; Freeman, L. V. D.; Goldwhite, H.; Rowsell, D. G. Phosphiran. *J. Am. Chem. Soc.* **1967**, *89*, 1102−1104.

(21) (a) Marinetti, A.; Mathey, F.; Fischer, J.; Mitschler, A. Generation and trapping of terminal phosphinidene complexes.

Synthesis and x-ray crystal structure of stable phosphirene complexes. *J. Am. Chem. Soc.* **1982**, *104*, 4484−4485. (b) Marinetti, A.; Mathey, F.; Fischer, J.; Mitschler, A. Synthesis and X-Ray Crystal Structure of 1,2,3-Triphenylphosphirene. *J. Chem. Soc., Chem. Commun.* **1984**, 45−46.

(22) Wagner, O.; Maas, G.; Regitz, M. Das erste 2*H*-Phosphiren. *Angew. Chem.* **1987**, *99*, 1328−1330; The first 2*H*-Phosphirene. *Angew. Chem. Int. Ed.* **1987**, *26*, 1257−1259.

(23) (a) Mathey, F. Phosphaorganische Chemie: Panorama und Perspektiven. *Angew. Chem.* **2003**, *115*, 1616−1643;Mathey, F. Phospha-Organic Chemistry: Panorama and Perspectives. *Angew. Chem., Int. Ed.* **2003**, *42*, 1578−1604. (b) Mathey, F. Comparisons between the chemistry of phosphirenes and silirenes. *Pure Appl. Chem.* **1987**, *59*, 993−998. (c) Mathey, F. Chemistry of 3-Membered Carbon-Phosphorus Heterocycles. *Chem. Rev.* **1990**, *90*, 997−1025. (d) Mathey, F.; Regitz, M. *Comprehensive Heterocyclic Chemistry I*;Katritzky, A. R.; Rees, C. W.; Scriven, E. F. V., Eds.; Pergamon, 1997; Vol. *1A*, pp 277−304. (e) Regitz, M. *Phosphorus-Carbon Heterocyclic Chemistry: The Rise of a New Domain*; Mathey, F., Ed.; Pergamon, 2001; pp 17−55. (f) Streubel, R.; Ostrowski, A.; Wilkens, H.; Ruthe, F.; Jeske, J.; Jones, P. G. Überraschende intramolekulare Folgereaktionen intermediärer Phosphacarbonyl-Ylid-Wolframkomplexe. *Angew. Chem.* **1997**, *109*, 409−413;Streubel, R.; Ostrowski, A.; Wilkens, H.; Ruthe, F.; Jeske, J.; Jones, P. G. Unexpected Intramolecular Reactions of Intermediate Phosphacarbonyl Ylide Tungsten Complexes. *Angew. Chem., Int. Ed.* **1997**, *36*, 378−381. (g) Streubel, R.; Kusenberg, A.; Jeske, J.; Jones, P. G. Thermisch induzierte Ringspaltung eines 2*H*-1,2-Azaphosphiren-Wolframkomplexes. *Angew. Chem.* **1994**, *106*, 2564−2566;Streubel, R.; Kusenberg, A.; Jeske, J.; Jones, P. G. Thermally Induced Ring Cleavage of a 2*H*-1,2-Azaphosphirene Tungsten Complex. *Angew. Chem., Int. Ed.* **1995**, *33*, 2427−2428.

(24) Galland, N.; Hannachi, Y.; Lanzisera, D. V.; Andrews, L. Theoretical study of structures, energetics and vibrational properties of BC_2H_3 species. *Chem. Phys.* **1998**, *230*, 143−151.

(25) Rey Planells, A.; Espinosa Ferao, A. Accurate Ring Strain Energy Calculations on Saturated Three-Membered Heterocycles with One Group 13−16 Element. *Inorg. Chem.* **2020**, *59*, 11503−11513.

(26) Chatt, J.; Duncanson, L. A. Olefin Co-ordination Compounds. *J. Chem. Soc.* **1953**, 2939−2947.

(27) (a) Bader, R. F. W. *Atoms in Molecules: A Quantum Theory*; Oxford University Press: Oxford, U.K., 1990. (b) Bader, R. F. W. A quantum theory of molecular structure and its applications. *Chem. Rev.* **1991**, *91*, 893−928. (c) *The Quantum Theory of Atoms in Molecules: From Solid State to DNA and Drug Design*; Matta, C. F.; Boyd, R. J., Eds.; Wiley-VCH: New York, 2007; pp 1−34. (d) Biegler-König, F.; Schönbohm, J.; Bayles, D. Software news and updates-AIM2000-A program to analyze and visualize atoms in molecules. *J. Comput. Chem.* **2001**, *22*, 545−559. (e) Biegler-König, F.; Schönbohm, J. Update of the AIM2000-program for atoms in molecules. *J. Comput. Chem.* **2002**, *23*, 1489−1494.

(28) (a) Ma, N. L.; Wong, M. W. A Theoretical Study of the Properties and Reactivities of Ketene, Thioketene, and Selenoketene. *Eur. J. Org. Chem.* **2000**, *2000*, 1411−1421. (b) Mawhinney, R. C.; Goddard, J. D. Assessment of density functional theory for the prediction of the nature of the oxirene stationary point. *J. Mol. Struct.: THEOCHEM* **2003**, *629*, 263−270.

(29) Grimme, S.; Brandenburg, J. G.; Bannwarth, C.; Hansen, A. Consistent structures and interactions by density functional theory with small atomic orbital basis sets. *J. Chem. Phys.* **2015**, *143*, No. 054107.

(30) Espinosa Ferao, A.; García Alcaraz, A. Benchmarking the inversion barriers in $\sigma^3\lambda^3$-phosphorus compounds: a computational study. *New J. Chem.* **2020**, *44*, 8763−8770.

(31) Espinosa Ferao, A.; Rey Planells, A.; Streubel, R. Between oxirane and phosphirane: the spring loaded oxaphosphirane ring. *Eur. J. Inorg. Chem.* **2021**, *2021*, 348−353.

(32) Wheeler, S. E.; Houk, K. N.; v R Schleyer, P.; Allen, W. D. A Hierarchy of Homodesmotic Reactions for Thermochemistry. *J. Am. Chem. Soc.* **2009**, *131*, 2547−2560.

(33) (a) Krahe, O.; Neese, F.; Streubel, R. The Quest for Ring Opening of Oxaphosphirane Complexes: A Coupled-Cluster and Density Functional Study of CH_3PO Isomers and Their $Cr(CO)_5$ Complexes. *Chem. - Eur. J.* **2009**, *15*, 2594−2601. (b) Espinosa, A.; Streubel, R. Computational studies on azaphosphiridines and the quest of how to effect ring-opening processes via selective bond activation. *Chem. - Eur. J.* **2011**, *17*, 3166−3178. (c) Espinosa, A.; Gómez, C.; Streubel, R. Single electron transfer-mediated selective endo- and exocyclic bond cleavage processes in azaphosphiridine chromium(0) complexes: a computational study. *Inorg. Chem.* **2012**, *51*, 7250−7256. (d) Albrecht, C.; Schneider, E.; Engeser, M.; Schnakenburg, G.; Espinosa, A.; Streubel, R. Synthesis and DFT Calculations of Spirooxaphosphirane Complexes. *Dalton Trans.* **2013**, *42*, 8897−8906. (e) Espinosa, A.; de las Heras, É.; Streubel, R. Oxaphosphirane-borane complexes: Ring strain and migratory insertion reactions. *Inorg. Chem.* **2014**, *53*, 6132−6140. (f) Villalba Franco, J. M.; Sasamori, T.; Schnakenburg, G.; Espinosa Ferao, A.; Streubel, R. Going for strain: synthesis of the first 3-imino-azaphosphiridine complexes and their surprising conversion into oxaphosphirane complex valence isomers. *Chem. Commun.* **2015**, *51*, 3878−3881. (g) Espinosa Ferao, A.; Streubel, R. Thiaphosphiranes and their complexes: systematic study on ring strain and ring cleavage reactions. *Inorg. Chem.* **2016**, *55*, 9611−9619. (h) Espinosa Ferao, A. Kinetic energy density per electron as quick insight into ring strain energies. *Tetrahedron Lett.* **2016**, *57*, 5616−5619.

(34) (a) Espinosa Ferao, A.; Rey Planells, A. CHNO isomers and derivatives - A computational overview *New J. Chem.* 2022, *46*, 5771−5778. (b) Rey, A.; Espinosa Ferao, A.; Streubel, R. Quantum Chemical calculations on CHOP derivatives−spanning the chemical space of phosphinidenes, phosphaketenes, oxaphosphirenes and COP^- isomers. *Molecules* **2018**, *23*, No. 3341.

(35) Budzelaar, P. H. M.; Kos, A. J.; Clark, T.; von Ragué Schleyer, P. Effects of Boron substituents in Borirenes, Boriranes and Boranes. The Energies of B-X bonds. *Organometallics* **1985**, *4*, 429−437.

(36) (a) George, P.; Trachtman, M.; Bock, C. W.; Brett, A. M. An alternative approach to the problem of assessing destabilization energies (strain energies) in cyclic hydrocarbons. *Tetrahedron* **1976**, *32*, 317−323. (b) Gordon, M. S. Ring Strain in Cyclopropane, Cyclopropene, Silacyclopropane, and Silacyclopropene. *J. Am. Chem. Soc.* **1980**, *102*, 7419−7422. (c) Naruse, Y.; Ma, J.; Inagaki, S. Relaxation of ring strain by introduction of a double bond. *Tetrahedron Lett.* **2001**, *42*, 6553−6556. (d) Bach, R. D.; Dmitrenko, O. Strain Energy of Small Ring Hydrocarbons. Influence of C−H Bond Dissociation Energies. *J. Am. Chem. Soc.* **2004**, *126*, 4444−4452. (e) Khoury, P. R.; Goddard, J. D.; Tam, W. Ring strain energies: substituted rings, norbornanes, norbornenes and norbornadienes. *Tetrahedron* **2004**, *60*, 8103−8112. (f) Bach, R. D.; Dmitrenko, O. The Effect of Carbonyl Substitution on the Strain Energy of Small Ring Compounds and Their Six-Member Ring Reference Compounds. *J. Am. Chem. Soc.* **2006**, *128*, 4598−4611. (g) Bach, R. D. Ring Strain Energy in the Cyclooctyl System. The Effect of Strain Energy on (3+2) Cycloaddition Reactions with Azides. *J. Am. Chem. Soc.* **2009**, *131*, 5233−5243.

(37) Goumans, T. P. M.; Ehlers, A. W.; Lammertsma, K.; Würthwein, E.-U. *Endo/exo* Preferences for Double Bonds in Three-Membered Rings Including Phosphorus Compounds. *Eur. J. Org. Chem.* **2003**, *2003*, 2941−2946.

(38) Gómez-Zavaglia, A.; Kaczor, A.; Cardoso, A. L.; Pinho e Melo, T. M. V. D.; Fausto, R. Substituent effects on the photolysis of methyl 2-carboxylate substituted aliphatic 2*H*-azirines. *J. Mol. Struct.* **2007**, *834−836*, 262−269.

(39) Gordon, M. S.; Koob, R. D. Relative Stability of Multiple Bonds to Silicon: An ab Initio Study of C_2SiH_4 Isomers. *J. Am. Chem. Soc.* **1981**, *103*, 2939−2944.

https://doi.org/10.1021/acs.inorgchem.2c00067
Inorg. Chem. 2022, 61, 6459−6468

(40) Wilson, P. J.; Tozer, D. J. A Kohn-Sham study of the oxirene-ketene potential energy surface. *Chem. Phys. Lett.* **2002**, *352*, 540−544.
(41) Espinosa Ferao, A. Kinetic energy density per electron as quick insight into ring strain energies. *Tetrahedron Lett.* **2016**, *57*, 5616−5619.
(42) (a) Brandhorst, K.; Grunenberg, J. How strong is it? The interpretation of force and compliance constants as bond strength descriptors. *Chem. Soc. Rev.* **2008**, *37*, 1558−1567. (b) Büschel, S.; Jungton, A.-K.; Bannenberg, T.; Randoll, S.; Hrib, C. G.; Jones, P. G.; Tamm, M. Secondary Interactions in Phosphane-Functionalized Group 4 Cycloheptatrienyl−Cyclopentadienyl Sandwich Complexes. *Chem. - Eur. J.* **2009**, *15*, 2176−2184. (c) Espinosa, A.; de las Heras, É.; Streubel, R. Oxaphosphirane-Borane Complexes: Ring Strain and Migratory Insertion/Ring-Opening Reactions. *Inorg. Chem.* **2014**, *53*, 6132−6140.
(43) Naruse, Y.; Inagaki, S. Relaxation of Ring Strains. In *Orbitals in Chemistry*; Springer, 2009; Vol. *289*, pp 265−291.
(44) (a) Pauling, L.; Wheland, G. W. The Nature of the Chemical Bond. V. The Quantum-Mechanical Calculation of the Resonance Energy of Benzene and Naphthalene and the Hydrocarbon Free Radicals. *J. Chem. Phys.* **1933**, *1*, 362−374. (b) Fishtik, I.; Datta, R. Aromaticity *vs* Stoichiometry. *J. Phys. Chem. A* **2003**, *107*, 10471−10476. (c) Mo, Y.; von Ragué Schleyer, P. An Energetic Measure of Aromaticity and Antiaromaticity Based on the Pauling−Wheland Resonance Energies. *Chem. - Eur. J.* **2006**, *12*, 2009−2020. (d) Lazzeretti, P. Ring currents. *Prog. Nucl. Magn. Reson. Spectrosc.* **2000**, *36*, 1−88. (e) Mitchell, R. H. Measuring Aromaticity by NMR. *Chem. Rev.* **2001**, *101*, 1301−1316. (f) Bird, C. W. A new aromaticity index and its application to five-membered ring heterocycles. *Tetrahedron* **1985**, *41*, 1409−1414. (g) Kruszewski, J.; Krygowski, T. M. Definition of aromaticity basing on the harmonic oscillator model. *Tetrahedron Lett.* **1972**, *13*, 3839−3842. (h) Krygowski, T. M. Crystallographic Studies of Inter- and Intramolecular Interactions Reflected in Aromatic Character of π-Electron Systems. *J. Chem. Inf. Comput. Sci.* **1993**, *33*, 70−78.
(45) von Ragué Schleyer, P.; Maerker, C.; Dransfeld, A.; Jiao, H. J.; van Eikema Hommes, N. J. R. Nucleus-independent chemical shifts: a simple and efficient aromaticity probe. *J. Am. Chem. Soc.* **1996**, *118*, 6317−6318.
(46) Alonso, M.; Poater, J.; Solà, M. Aromaticity changes along the reaction coordinate connecting the cyclobutadiene dimer to cubane and the benzene dimer to hexaprismane. *Struct. Chem.* **2007**, *18*, 773−783.
(47) (a) Espinosa, A.; Frontera, A.; García, R.; Soler, M. A.; Tárraga, A. Electrophilic behaviour of 3-methyl-2-methylthio-1,3,4-thiadiazolium salts: A multimodal theoretical approach. *ARKIVOC* **2005**, *2005*, 415−437. (b) Gese, A.; Akter, M.; Schnakenburg, G.; García Alcaraz, A.; Espinosa Ferao, A.; Streubel, R. P-Functionalized tetrathiafulvalenes from 1,3-dithiole-2-thiones? *New J. Chem.* **2020**, *44*, 17122−17128.
(48) Compare with NICS(1) = −10.22 ppm and NICS(2) = −4.91 ppm computed for benzene at the same level.
(49) $\mathbf{1}^{As}$ (3.00 kcal/mol, 71.9% d-character), $\mathbf{1}^{Sb}$ (2.00 kcal/mol, 65.0% d-character), $\mathbf{1}^{Bi}$ (1.36 kcal/mol, 49.0% d-character) $\mathbf{1}^{Se}$ (3.56 kcal/mol, 48.4% d-character), $\mathbf{1}^{Te}$ (2.99 kcal/mol, 47.3% d-character) and $\mathbf{1}^{Po}$ (2.11 kcal/mol, 39.1% d-character).
(50) (a) Nyulászi, L.; Benkő, Z. Three-Membered Rings with two Heteroatoms Including Selenium or Tellurium; Three-Membered Rings with Three Heteroatoms. In *Comprehensive Heterocyclic Chemistry III*; Elsevier, 2008. (b) Nyulászi, L.; Benkő, Z. Aromatic Phosphorus Heterocycles. In *Topics in Heterocyclic Chemistry*; Springer, 2009; Vol. *19*, pp 27−81. (c) Hajgató, B.; De Proft, F.; Szieberth, D.; Tozer, D. J.; Deleuze, M. S.; Geerlings, P.; Nyulászi, L. Bonding in negative ions: the role of d orbitals in the heavy analogues of pyridine and furan radical anions. *Phys. Chem. Chem. Phys.* **2011**, *13*, 1663−1668.
(51) Wiberg, K. B. Application of the pople-santry-segal CNDO method to the cyclopropylcarbinyl and cyclobutyl cation and to bicyclobutane. *Tetrahedron* **1968**, *24*, 1083−1096.
(52) Reed, A. E.; Weinhold, F. Natural localized molecular orbitals. *J. Chem. Phys.* **1985**, *83*, 1736−1740.
(53) Outeiral, C.; Vincent, M. A.; Pendás, Á. M.; Popelier, P. L. A. Revitalizing the concept of bond order through delocalization measures in real space. *Chem. Sci.* **2018**, *9*, 5517−5529.
(54) The multi-reference RSE calculation for $\mathbf{2}^{As*}$ was obtained only from the C═El and C-C bond cleavage homodesmotic reactions, due to convergence problems in the other (C-El bond cleavage) homodesmotic reaction.
(55) Neese, F. *ORCA - An Ab initio, DFT and Semiempirical SCF-MO Package*, version 4.2.1; Max Planck Institute for Bioinorganic Chemistry, 2019.
(56) (a) Lee, C.; Yang, W.; Parr, R. G. Development of the Colle-Salvetti correlation energy formula into a functional of the electron density. *Phys. Rev. B.* **1988**, *37*, 785−789. (b) Becke, A. D. Density-functional thermochemistry. III. The role of exact Exchange. *J. Chem. Phys.* **1993**, *98*, 5648−5652.
(57) Weigend, F.; Ahlrichs, R. Balanced basis sets of split valence, triple zeta valence and quadruple zeta valence quality for H to Rn: Design and assessment of accuracy. *Phys. Chem. Chem. Phys.* **2005**, *7*, 3297−3305.
(58) Grimme, S.; Antony, J.; Ehrlich, S.; Krieg, H. A consistent and accurate ab initio parametrization of density functional dispersion correction (DFT-D) for the 94 elements H-Pu. *J. Chem. Phys.* **2010**, *132*, No. 154104.
(59) (a) Schafer, A.; Huber, C.; Ahlrichs, R. J. *Chem. Phys.* 1994, *100*, 5829−5835, basis sets may be obtained from the Basis Set Exchange (BSE) software and the EMSL Basis Set Library: https://bse.pnl.gov/bse/portal. (b) Feller, D. The Role of Databases in Support of Computational Chemistry Calculations. *J. Comput. Chem.* **1996**, *17*, 1571−1586.
(60) Riplinger, C.; Sandhoefer, B.; Hansen, A.; Neese, F. Natural triple excitations in local coupled cluster calculations with pair natural orbitals. *J. Chem. Phys.* **2013**, *139*, No. 134101.
(61) Pople, J. A.; Head-Gordon, M.; Raghavachari, K. Quadratic configuration interaction. A general technique for determining electron correlation energies. *J. Chem. Phys.* **1987**, *87*, 5968−5975.
(62) Roos, B. O. The Complete Active Space Self-Consistent Field Method and its Applications in Electronic Structure Calculations. In *Advances in Chemical Physics*; John Wiley & Sons, 1987; pp 399−445.
(63) Gdanitz, R. J.; Ahlrichs, R. The averaged coupled-pair functional (ACPF): A size-extensive modification of MR CI(SD). *Chem. Phys. Lett.* **1988**, *143*, 413−420.
(64) Rappoport, D.; Furche, F. Property-optimized Gaussian basis sets for molecular response calculations. *J. Chem. Phys.* **2010**, *133*, No. 134105.
(65) (a) Reed, A. E.; Weinhold, F. Natural bond orbital analysis of near-Hartree−Fock water dimer. *J. Chem. Phys.* **1983**, *78*, 4066−4073. (b) Reed, A. E.; Weinstock, R. B.; Weinhold, F. Natural population analysis. *J. Chem. Phys.* **1985**, *83*, 735−746.
(66) Lu, T.; Chen, F. Multiwfn: A Multifunctional Wavefunction Analyzer. *J. Comput. Chem.* **2012**, *33*, 580−592.
(67) Keith, T. A. *AIMAll*, Ver. 14.06.21; TK Gristmill Software: Overland Park, Kansas, U.S.A., aim.tkgristmill.com, 2014.
(68) Humphrey, W.; Dalke, A.; Schulten, K. VMD: Visual molecular dynamics. *J. Mol. Graphics* **1996**, *14*, 33−38.

https://doi.org/10.1021/acs.inorgchem.2c00067
Inorg. Chem. 2022, 61, 6459−6468